The performance of slender monuments during the 2015 Gorkha earthquake

Anjali Mehrotra[a)] and Matthew DeJong[a)] M.EERI

This paper studies damage to a few specific monuments in the Kathmandu Valley which were either partially or completely destroyed during the 2015 Gorkha earthquake. Three of these structures - namely the Basantapur Column, the Dharahara Tower, and the Narayan Temple - were modelled both analytically using rocking dynamics, and computationally using discrete element modelling. The results emphasize the importance of large low-frequency content within the ground motion, demonstrating that the Dharahara tower could have collapsed due to the primary long-period ground motion pulse alone. In addition, comparison of analytical and computational modelling to the observed response enables evaluation of structural behavior, including discussion of the importance of elastic amplification and column embedment on performance during the earthquake.

INTRODUCTION

The 2015 Nepal earthquake caused a significant amount of damage in the Kathmandu Valley – leaving over 8,790 dead, 22,300 injured, and in total affecting 8 million people - almost a third of Nepal's population (National Planning Commission (NPC) 2015). Economic losses were also catastrophic and were estimated to be approximately $7 billion – or a third of Nepal's GDP (National Planning Commission (NPC) 2015). The earthquake also caused severe structural damage to many buildings and other constructions in the Kathmandu Valley. However, unlike the 1934 Nepal-Bihar earthquake, which destroyed about 20% of the vernacular dwellings in Kathmandu, less than 1% of these structures were destroyed during the earthquake in 2015 (Galetzka et al. 2015), with most destruction being limited to low-strength stone and brick masonry structures, while many reinforced concrete buildings sustained little to no harm (Goda et al. 2015). Furthermore, taller masonry structures were observed to have been more adversely affected by the earthquake, with structures such as Kathmandu's iconic Dharahara Tower completely collapsing, despite partially surviving the earthquake in 1934 (Galetzka et al. 2015).

[a)] Department of Engineering, University of Cambridge, United Kingdom

Previous studies have generally focused on geotechnical aspects of the earthquake and characteristics of the ground motion, and comprise mostly field observations and damage surveys (Aydan and Ulusay 2015; Goda et al. 2015; Dixit et al. 2015; Hayes et al. 2015; Martin, Hough, and Hung 2015; Galetzka et al. 2015). However recent work by Parajuli & Kiyono (2015) also included field tests to determine local material properties such as the compressive strength of brick and stone masonry, as well as the coefficient of friction and the cohesive strength of mud mortar, while Tallet-Williams et al. (2016) investigated the influence of site-amplification in the Kathmandu Valley.

The primary objective of this paper is to evaluate the behavior of slender monuments during the 2015 Gorkha earthquake – in particular, to assess the effects of scale, slenderness and pulse duration on the dynamic response of these structures. While previously-conducted studies (Housner 1963; Yim, Chopra, and Penzien 1980; Makris and Roussos 2000 etc) have already established that, in general, larger structures are more resistant to overturning, slender structures are less resistant, and longer period pulses are more capable of causing collapse, this paper aims to quantify these effects in a more detailed manner using a few case-study monuments which collapsed during the earthquake in 2015.

The selected monuments comprise a column topped with a statue of the Hindu god Garuda in the Basantapur Durbar Square (referred to here as the Basantapur Column (Figure 1a)), the Dharahara Tower in Kathmandu (Figure 1b), and the Narayan Temple in Bhaktapur (Figure 1c). These particular monuments were chosen as they are relatively simple, symmetric, and of considerably varying size. The structures were modelled both analytically using rocking dynamics and computationally using discrete element modelling (DEM) in 3DEC, which is a 3D numerical modelling tool that simulates the dynamic response of discontinuous materials such as masonry by representing them as an assemblage of discrete rigid or deformable blocks which interact through contact elements (joints) (Itasca Consulting Group 2007). As it can model large displacements and rotations between individual blocks, DEM can be used to predict the more complex behavior of multi-block structures which might not always be captured by the simplified analytical models. Thus in this paper, DEM in 3DEC will be used to not only evaluate simplifications made in the analytical models but also investigate the influence of certain parameters on the structures' dynamic response that cannot be captured analytically.

Figure 1. (a) Basantapur Column (Source: Alamy/AP), (b) Dharahara Tower before and after the 2015 earthquake (Source: Ian Trower/JAI/Corbis & Narendra Shrestha/EPA) and (c) Narayan Temple after the earthquake and corresponding cracking mechanism.

ANALYTICAL MODELLING

Analytical modelling was conducted using rocking dynamics, following methods developed by Housner (1963), as the seismic collapse of unreinforced masonry structures is often governed by large displacement dynamics rather than the linear elastic response, or even small displacement inelastic behavior. As failure typically occurs via specific collapse mechanisms, their nonlinear behavior can be captured by deriving and solving equations of motion for the given collapse mechanism which may exhibit rocking behavior.

Early work on rocking (Housner 1963) derived these equations of motion for simple structures whose geometry could be approximated by a single rocking block. These equations of motion have been solved for full time-histories of various major earthquakes to generate rocking spectra (Makris and Zhang 1999; Makris and Konstantinidis 2001), which illustrate the relationship between size, slenderness and overall stability of rocking blocks.

Zhang & Makris (2001) built upon Housner's work by studying the rocking response of rigid blocks to pulse-type excitations, which were used to approximate near-source ground motion and often govern overturning collapse. Closed-form solutions to Housner's equation of motion for a single rocking block when subjected to cycloidal pulses were derived by Dimitrakopoulos & DeJong (2012), who also provided analytical equations for non-dimensional overturning plots, so that the nonlinear response of the block to any pulse-type excitation could be easily-determined – needing only to be scaled by the intensity and frequency of the ground motion. Equations of motion were also derived for structures with non-rectangular geometries, such as stone spires (DeJong 2012b). DeJong & Dimitrakopoulos (2014) then proposed to linearize the equations of motion of more complicated multiple-block rocking mechanisms to enable single rocking block solutions to

approximate the rocking dynamics of any of the typically catalogued masonry collapse mechanisms.

In this section, rocking dynamics is used to analytically model the behavior of three simple monuments - the Basantapur Column and Dharahara Tower in Kathmandu, as well as the Narayan Temple in Bhaktapur– all of which sustained varying levels of damage during the Gorkha earthquake in 2015. Equations of motion are derived for each of the collapse mechanisms, and solved for both full time-histories as well as cycloidal pulses to generate overturning plots, with the latter being used to rapidly compare the relative dynamic resilience of the different structures.

METHODOLOGY

Equations of motion

The derivation of the equations of motion for the considered monuments/collapse mechanisms was conducted using an approach similar to that proposed by Housner (1963). Assuming that the selected structures rock back and forth on their bases and no bouncing or sliding occurs, their rocking response to seismic excitation can be described by the following generalized equations of motion:

$$I_0\ddot{\theta} + MgR\sin\left(+\alpha-\theta\right) = -M\ddot{u}_g R\cos\left(+\alpha-\theta\right) \rightarrow \theta > 0 \quad (1)$$

$$I_0\ddot{\theta} + MgR\sin\left(-\alpha-\theta\right) = -M\ddot{u}_g R\cos\left(-\alpha-\theta\right) \rightarrow \theta < 0 \quad (2)$$

where I_0 is the moment of inertia of the collapsed portion of the structure about the axis of rotation, M is the total mass, R is the distance between the center of mass and the rotation axis, α is the critical angle (and the slenderness of the structure), θ is the rocking rotation and $\ddot{u}_g$ is the horizontal ground acceleration. With the exception of $\ddot{u}_g$, all the other terms in the equation are based solely on the geometry of the structure, with rocking initiating when $\ddot{u}_g \geq g\tan(\alpha)$. In the case of slender structures ($\alpha \leq 0.35$ rad, (Housner 1963)), Equations 1-2 can also be linearized about the point of unstable equilibrium ($\theta = \alpha$) and be rewritten as:

$$\ddot{\theta} = -p^2\left(\frac{\ddot{u}_g}{g} + \alpha - \theta\right) \rightarrow \theta > 0 \quad (3)$$

$$\ddot{\theta} = -p^2\left(\frac{\ddot{u}_g}{g} - \alpha - \theta\right) \rightarrow \theta < 0 \quad (4)$$

where p is the rocking frequency parameter and is equal to $\sqrt{MgR/I_0}$.

Furthermore, in order to account for the energy dissipated during impact, a coefficient of restitution η is also defined, which is assumed to be a function of the geometry of the structure and is determined using conservation of moment of momentum about the axis of rotation (Housner 1963). In the case of two-sided rocking (assumed for all three monuments), this coefficient of restitution is thus calculated using the following expression:

$$\eta = 1 - 2\frac{p^2 R}{g}\sin^2\alpha \tag{5}$$

Rhino models and script

The kinematic constants (namely the rocking frequency parameter p, the slenderness α and the coefficient of restitution η) defining the equations of motion presented above, were derived using scripts written in Rhino, which automatically calculate these parameters for any user-defined structural geometry/mechanism. As input, the scripts require CAD files of the structures under consideration, which in this case were generated using survey data taken by hand (for the Basantapur column) and laser scanning (for the Dharahara Tower and the Narayan Temple).

As the statue at the top of the Basantapur column had been removed almost immediately after the earthquake, its dimensions had to be estimated using photographs and it was thus recreated using simple geometries in Rhino, as illustrated by a. The entire structural geometries of the Dharahara Tower and the Narayan Temple, on the other hand, were reconstructed in Rhino using point cloud data from the laser scanner, with this data also allowing the collapse mechanisms of the tower and temple to be easily determined.

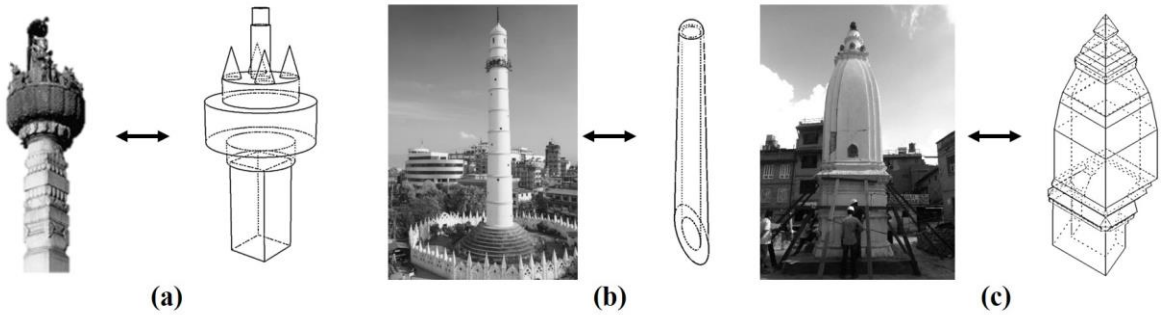

Figure 2. Rhino models of the collapsed portions of the (a) Basantapur Column, (b) Dharahara Tower and (c) Narayan Temple.

The Rhino script was then run for each of the different monuments/mechanisms. As input, upon opening the CAD file and calling the script, the user was prompted to select all

the objects involved in the mechanism and define the axis of rotation as well as any cracks which occur. Based on this input alone, the script then automatically calculated the resulting kinematic constants (Table 1), which were exported to Matlab to generate and solve the equations of motion for the given mechanisms.

Table 1. Kinematic constants derived for each of the different monuments

Structure	p^2 (s^{-2})	α (rad)	η
Basantapur Column	4.24	0.16	0.96
Dharahara Tower	0.25	0.12	0.98
Narayan Temple	1.93	0.24	0.91

Ground Motion

The equations of motion exported to Matlab were solved for the full acceleration time-history of the Nepal earthquake using the ground motion records from the USGS KATNP station in Kathmandu, as well as from the Bhaktapur (THM) and Patan (PTN) stations of Hokkaido University and Tribhuvan University (Takai et al. 2016), in both the east-west (EW) and north-south (NS) directions. The KATNP station was located approximately 1.2 km and 1.4 km away from the Basantapur Column and Dharahara Tower respectively, and 12 km away from the Narayan Temple. As Figure 3 illustrates, the ground motion recorded at this station was characterized by distinct high amplitude, low frequency pulses with periods of approximately 5 s and PGAs of 1.55 m/s^2 and 1.61 m/s^2, accompanied by relatively large ground displacements of 1.17 m and -1.39 m in the EW and NS directions respectively. The THM station, on the other hand, was located approximately 7.1 km and 6.5 km away from the Basantapur Column and Dharahara Tower respectively, and 5.4 km away from the Narayan Temple. The ground motion recorded at this station had a number of distinct pulses, with periods of approximately 4 s and PGAs of 1.34 m/s^2 and 1.42 m/s^2 in the EW and NS directions respectively (Figure 3). Similarly, the PTN station was found to be 2.7 km, 2.1 km and 10.7 km away from the Basantapur Column, Dharahara Tower and Narayan Temple respectively. However the ground motion recorded at this station was characterized by higher frequency pulses and lower PGAs, with an average pulse period of approximately 3.5 s and PGAs of 1.28 m/s^2 and 1.51 m/s^2 in the EW and NS directions respectively (Figure 3).

The full time-history response of each of the monuments (for different levels of scaling of the acceleration records) was measured in terms of the maximum rotation of the structure over time, with the rotation θ being expressed as a fraction of the critical angle (and slenderness) α and overturning generally occurring when this ratio exceeded 1.

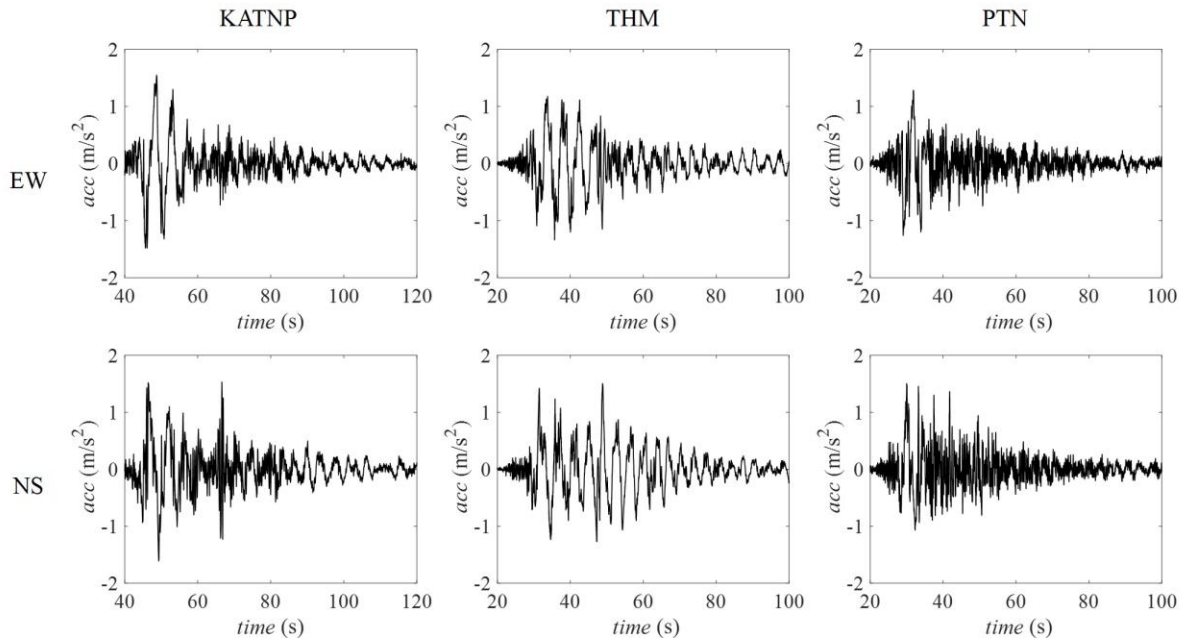

Figure 3. Input ground motion as recorded at the USGS Kathmandu (KATNP), Bhaktapur (THM) and Patan (PTN) stations, in both the East-West (top) and North-South (bottom) directions (Takai et al. 2016).

Overturning envelopes (Dimitrakopoulos & DeJong 2012) were also generated for each of the structures and were used to predict the response of the monuments to the primary sine pulses (characterized by a frequency f_p and pulse amplitude a_p) isolated from the earthquake ground motion records. Each pulse is represented as a singular point on the overturning plot, and depending on which region of the plot it lies in, it is predicted to either cause no rocking, rocking but no overturning, overturning with impact, or overturning without impact. Furthermore, as the ground motion scaling (and consequently the isolated pulse amplitude a_p) increases, this point moves up in the plot – gradually migrating from the "safe" (no rocking/overturning) zone to the "unsafe" (overturning) zone. While this comparison does not account for the potential amplifying/de-amplifying effect of the remainder of the ground motion, it does however allow for rapid prediction of the proportion of the response that could be caused by the single maximum pulse alone.

RESULTS

While all three structures were subjected to the six ground motion records shown in Figure 3, the results presented here are only for the ground motion recorded at the station closest to each site (in the dominant direction of collapse), which in the case of the Basantapur Column and the Dharahara Tower, was USGS KATNP station in Kathmandu, and in the case of the Narayan Temple, the THM station in Bhaktapur.

Basantapur Column

As collapse of the Basantapur Column occurred towards the east, the results presented here are for the EW component of the KATNP ground motion. In the case of this structure, the time-history results (Figure 4a) predicted overturning of the column for scaling factors of 1.15 and higher, with overturning generally occurring when θ/α exceeded an absolute value of 1. For lower levels of scaling of the earthquake ground motion, the column was found to rock with multiple impacts before returning to equilibrium – indicating that the scaled acceleration was large enough to initiate rocking, but not large enough to cause collapse. For scaling factors of 1.15 to 1.25, the column rocked with multiple impacts before overturning, while for larger scaling factors the column overturned without impact. Moreover, while the time required for collapse generally decreased with an increase in ground motion scaling, overturning was actually observed to occur faster for the scaling factor of 1.15 than for the higher scaling factors of 1.20 and 1.25.

An overturning plot (Figure 4b) was also generated, including the primary pulses isolated from the scaled acceleration records. To facilitate comparison with the time-history results, these pulses were plotted using filled circles (•) for cases where the time-history plots predicted collapse, and crosses (x) for cases where they did not. In general, good agreement was observed between both sets of results, with the overturning plot usually providing more conservative predictions – as was the case for the scaling factor of 1.10, where the overturning plot predicted collapse while the time-history indicated a return to equilibrium.

Dharahara Tower

As collapse of the Dharahara Tower was observed to have occurred in a roughly south-western direction, ideally the results presented here would be for both the EW and NS components of the KATNP ground motion. However, in the interest of brevity only the NS time-history results (Figure 5**Error! Reference source not found.**a) are presented here, while the overturning plot generated for the tower contain pulses isolated from both components of the ground motion. In the case of the time-history results, collapse of the tower was generally found to occur for scaling factors of 1.50 and higher, with the exception of the scaling factor of 1.15, which was found to cause overturning as well.

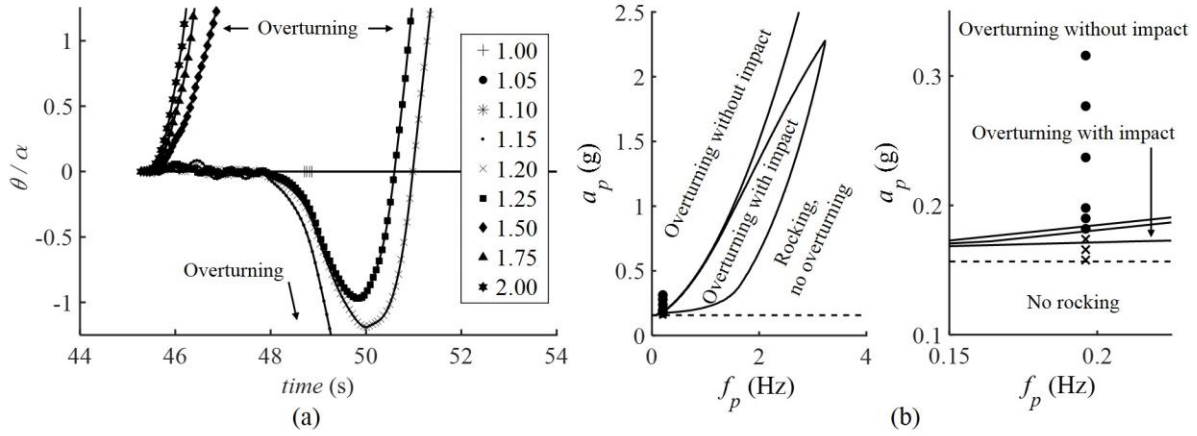

221

222 **Figure 4.** Basantapur Column: (a) Time-history responses for ground motion scaling values shown;
223 (b) Overturning envelope (right figure is zoomed view of left) for same ground motion scaling values

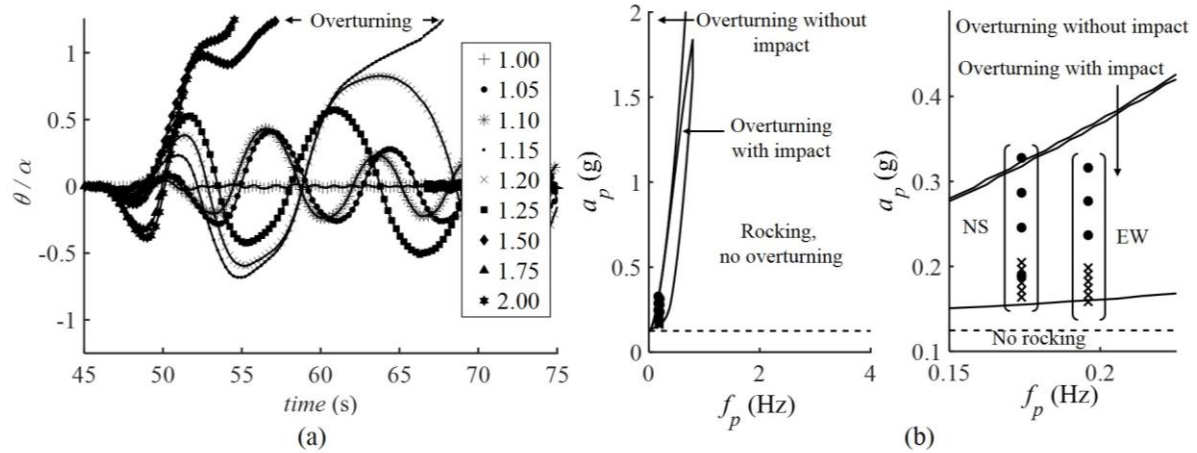

224

225 **Figure 5.** Dharahara Tower: (a) Time-history responses for ground motion scaling values shown; (b)
226 Overturning envelope (right figure is zoomed view of left) for same ground motion scaling values

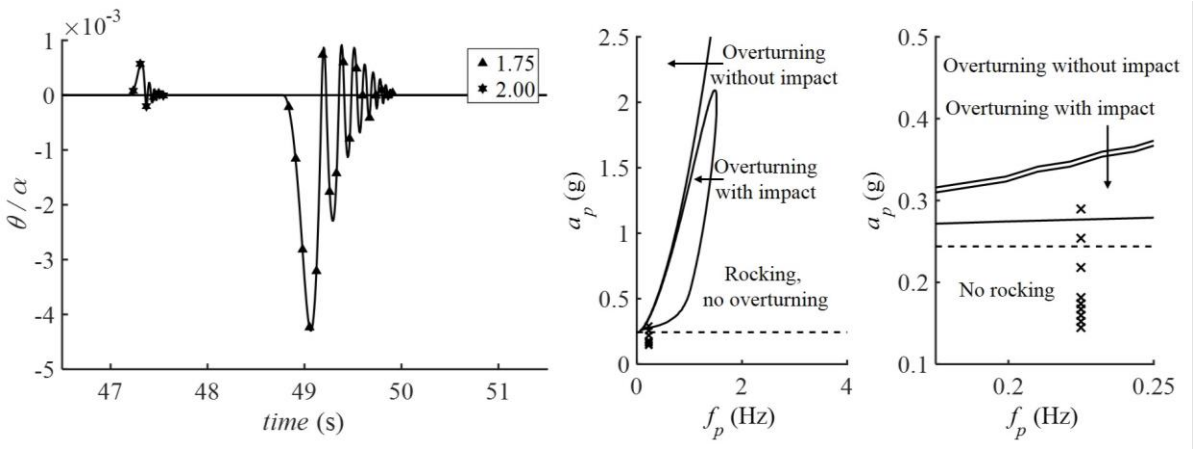

227

228 **Figure 6.** Narayan Temple: (a) Time-history responses for ground motion scaling values shown; (b)
229 Overturning envelope (right figure is zoomed view of left) for same ground motion scaling values

For scaling factors of 1.50 and higher, the tower was found to rock with a single impact before collapsing – comparing quite well with the mode of failure predicted by the overturning plots (Figure 5**Error! Reference source not found.**b). For the scaling factor of 1.15, the tower was observed to rock with multiple (3) impacts before overturning indicating that more than a single sine pulse must be considered in order to predict the response (see Discussion). For ground motion scaling of 1.05 times and higher, the tower was found to experience rocking amplitudes greater than $\theta/\alpha = 0.4$, and rock with multiple impacts before returning to equilibrium. It is noteworthy, that although complete rigid body collapse is not predicted, the Italian building code (NTC 2008) specifies a value of $\theta/\alpha = 0.4$ when predicting collapse of out-of-plane mechanisms in URM structures. Thus these very large rotation values indicate that if material failure and geometric imperfections were considered, collapse may well still occur. Fairly similar behavior was observed in the case of the East-West time-histories (not shown), with overturning occurring for scaling factors of 1.50 and higher.

Unlike the Basantapur Column, the predictions of the overturning plots of Dharahara Tower had far more inconsistencies with their time-history counterparts, with the former once again yielding more conservative results. Moreover, dashed lines demarcating the threshold acceleration below which no rocking occurs were added to each of the overturning plots and it can be seen that in the case of the columns in particular, the region in which the structures go from no rocking at all to complete overturning is extremely small – highlighting the importance of the long pulse present in the Nepal earthquake ground motion.

Narayan Temple

As the principal axis of the Narayan Temple is oriented along the NNE-SSW direction, and the main cracks were observed to occur on the southeastern façade (Menon et al. 2017), the results presented here are for the NS component of the ground motion recorded at the THM station. From the time-history results (Figure 6a) it can be seen that rocking of the structure only initiates for scaling factors of 1.75 and higher, while overturning of the structure does not occur for any of the considered scaling factors. For both the scaling factors of 1.75 and 2.00, the temple undergoes low-amplitude, high-frequency rocking before returning to equilibrium. In fact, the maximum rotation experienced by the temple is for the scaling factor of 1.75, and corresponds $\theta/\alpha \approx 0.004$. However, this small rotation is still most likely an overestimate, as the assumption of two-sided rocking for the temple is conservative

– in fact, two-sided rocking would require formation of the identical mechanism in the opposite direction, which would result in far more energy dissipation than is assumed here.

An overturning plot was also generated for the temple and the primary pulses isolated from the scaled acceleration records were plotted on it (Figure 6b). In general, a fairly good correlation was observed between the predictions of the overturning plot and the time-history results, with the exception of the scaling factor of 2 - for which the overturning plot predicted collapse while the time-history indicated a return to equilibrium.

In order to compare the responses of the three structures to the ground motion recorded at each of the different stations, bar graphs were also generated showing the minimum scaling factors required for rocking to initiate (Figure 7a) and overturning to occur (Figure 7b) for each structure, for each of the acceleration records provided in Figure 3. From Figure 7a it can be seen that the Dharahara Tower (DT), being the most slender, starts rocking for lower scaling factors than either the Basantapur Column (BC) or Narayan Temple (NT). Nevertheless once rocking initiates, the Basantapur Column, due to its smaller size, generally overturns for lower scaling factors than either the tower or the temple (Figure 7b).

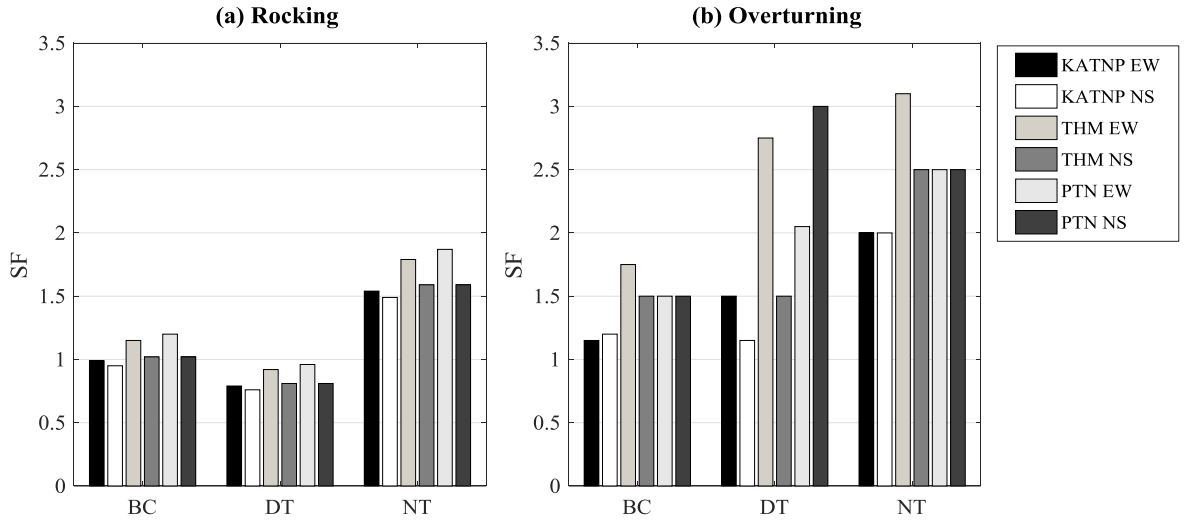

Figure 7. Scaling factors required to (a) initiate rocking and (b) cause overturning of each of the three structures, for the different ground motion records.

DISCRETE ELEMENT ANALYSIS

While the analytical models provide a very quick and computationally-inexpensive way of modelling the global seismic response of the selected monuments, they are not capable of predicting the more complicated features of dynamic collapse of multi-block structures, which can be influenced by block stereotomy and local block displacements (DeJong and

Vibert 2012). Thus computational analyses were also conducted using discrete element modelling (DEM) in 3DEC to investigate certain aspects of the dynamic response not considered by the simplified analytical models.

DEM can be used to model the large displacement response of masonry structures as it inherently captures discrete body interaction and allows for joint contact recognition in a more efficient manner than many finite element modelling procedures. The suitability of DEM for modelling both the static and dynamic behavior of masonry structures has been validated through several studies, with the tested structures comprising unreinforced masonry walls (Bui and Limam 2012; de Felice and Giannini 2000), free-standing columns (Papastamatiou and Psycharis 1993; Papantonopoulos et al. 2002), arches (Roberti and Calvetti 1998; De Lorenzis, DeJong, and Ochsendorf 2007; Mehrotra, Arêde, and DeJong 2015) and stone spires (DeJong and Vibert 2012), amongst others.

In this section, discrete element analysis will be used in 3DEC to computationally model the seismic response of the Basantapur Column and the Dharahara Tower to the Nepal earthquake ground motion. In addition to validating the analytical results, parametric studies are also conducted to assess the influence of factors such as the column embedment depth and joint stiffness, and in the case of the Dharahara Tower the effect of the pedestal and joint tensile strength, on the dynamic response.

METHODOLOGY

Basantapur Column

The 3DEC model of the Basantapur Column was directly generated from the CAD file created for the analytical modelling of the structure. Rigid blocks were used in the analysis, and their material properties were assumed to be those of stone for the column itself and bronze for the statue on top (see Table 2). The joint stiffnesses were calculated individually for each joint based on the Young's modulus of the materials involved and the distance between the interfaces. A friction angle of 35° was specified for all joints, which falls within the range of values reported in Barton (1976) for rock joints, except at the base where a larger angle of 80° was adopted to account for the presence of the tenon and mortise joints observed on site. The joints were also assumed to have no tensile strength or cohesion, as the column was made of dry stone masonry with no mortar.

Table 2. Block material properties

Property	Stone	Bronze	Brick
Density, ρ (kg/m^3)	2300	8700	2000
Young's modulus, E (GPa)	45	108	4.75
Poisson's ratio, υ	0.25	0.34	0.25

Stiffness-proportional Rayleigh damping was used for the dynamic simulations in order to damp out the influence of unrealistic high-frequency vibrations (DeJong 2009), with a damping constant of 1.96 x 10^{-4} being specified. For both the column and the Dharahara Tower, the earthquake loading was applied simultaneously in both cardinal directions using the acceleration data from the KATNP station in Kathmandu (Figure 3). The vertical component of the ground motion was not applied, as its influence is practically negligible for heavier blocks (Gazetas et al. 2012). Furthermore, as dynamic analyses can be computationally expensive and fairly time-intensive, the analyses in 3DEC were run for the first 20 seconds of the record, beyond which the ground motion was so small that it was found to have a negligible effect on the results.

In the first set of analyses, the base columns were assumed to be embedded deep enough into the ground that they could be treated as fixed (Figure 8a) – which was also the assumption made in the analytical models (see results in Figure 4). The results from these analyses were thus used to validate the predictions of the analytical models. The second set of analyses used the Basantapur Column to investigate the influence of the column embedment depth and joint stiffness at the embedment on the stability of the structure. In order to do this, the base column was no longer assumed to be fixed and the 4.6 m of the column visible above the ground was kept constant, while the length of the column below the ground was varied from 25% to 75% of the length above ground (Figure 8**Error! Reference source not found.**b). Furthermore, the joint stiffness calculated at the embedment was divided by factors of 1, 10 and 100 in order to simulate different soil conditions and gauge how the softening of the joints at the base affects the response of the structure. The ground motion in this case was not scaled as the objective was to evaluate the responses by comparing the maximum rocking rotation.

Dharahara Tower

The 3DEC model for the Dharahara Tower was also generated using the CAD file created for the analytical modelling. However, unlike the columns which were made up of a few individual large blocks which could directly be modelled in 3DEC, the brick masonry

tower was discretized into relatively large blocks to decrease computation time. Thus the shaft of the tower was divided into twenty 3.0 m high layers, with each layer containing 12 blocks joined in pairs of two in such a manner as to ensure some degree of interlocking over the height of the structure. The widths and thicknesses of the individual blocks making up each layer gradually decreased in line with the tapering form of the tower. The final discretized geometry is illustrated in Figure 8**Error! Reference source not found.**c.

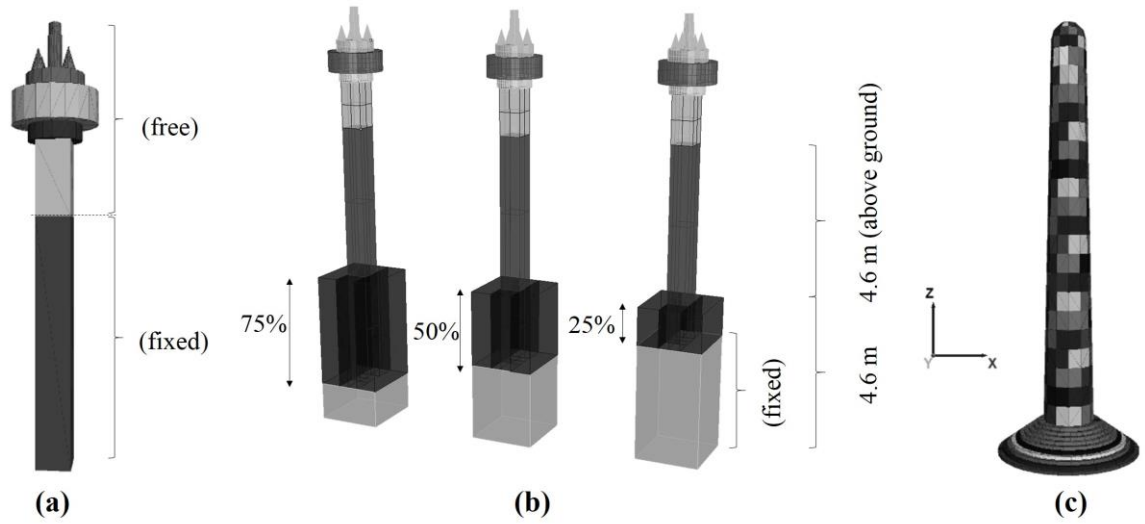

Figure 8. (a) Fixed base column 3DEC models; (b) Embedded base column 3DEC models; (c) Dharahara Tower 3DEC model (final discretized geometry)

Rigid blocks were once again used in the analysis. Typical material properties of clay brick masonry with lime *surkhi* mortar were assumed for the tower (Table 2, Rai and Dhanapal (2013), Kaushik, Rai, and Jain (2007)), while typical properties of stone were assumed for the pedestal upon which the tower sits. The joint stiffnesses were calculated based on the Young's moduli of the interface materials and the distance between joints, while a minimal joint tensile strength of 1.00 kPa was assumed in order to account for the mortar as well as eliminate disintegration throughout the tower and thus more realistically model its collapse – although the magnitude of this tensile strength was later varied in order to gauge its effect on the response of the structure. A friction angle of 35°, which falls within the range of values determined experimentally by Atkinson et al. (1989), Drysdale, Vanderkeyl, and Hamid (1979), Stockl and Hofmann (1986) and Capozucca (2011) for clay brick masonry with mortar, was defined for all the joints. Parametric studies were also conducted to analyze the effect of ground motion scaling on the tower's dynamic response, as well as the influence of the pedestal. Stiffness-proportional damping was again used for the dynamic analysis, with a damping constant of 1.85×10^{-4} being specified for the structure.

RESULTS

Basantapur Column

Fixed base column model

In the case of the Basantapur Column, the fixed base column model was used for comparison with the predictions of the analytical model. In general it was found that the collapsed portions of the column did not behave as multiple sliding and rocking surfaces, and instead rocked monolithically – thereby confirming the simplified assumptions of the analytical model. To better facilitate comparison with the analytical results, the time-history responses of the computational model were plotted in terms of the variation of the maximum rotation of the column over time, with the rotation being expressed as a fraction of the critical angle α. As Figure 9 illustrates, the analytical and computational results were observed to be in fairly good agreement for the ground motion scaling levels shown.

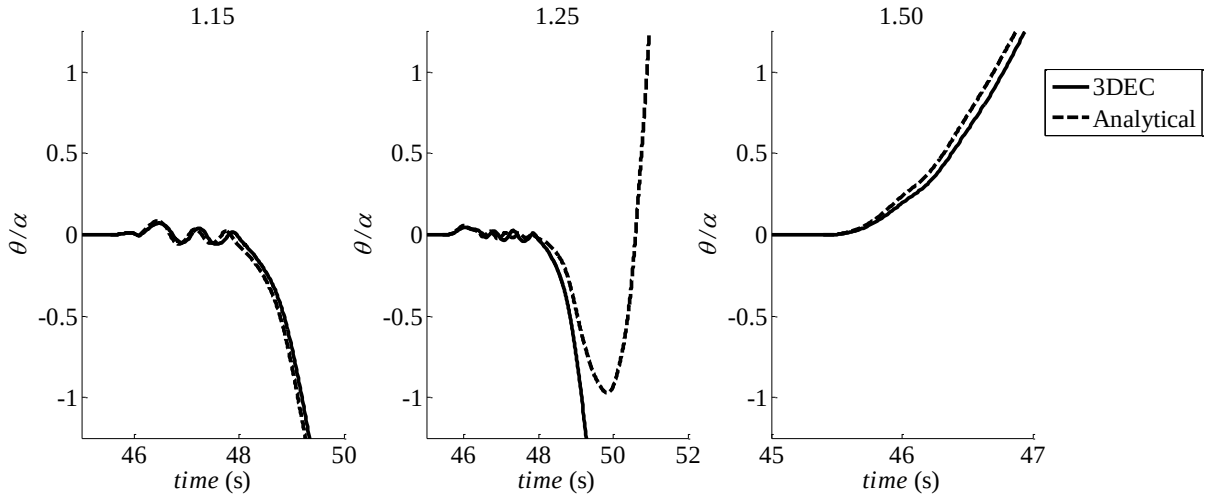

Figure 9. Comparison between 3DEC and analytical time-history results for the Basantapur Column

Embedded column model

The second set of analyses conducted on the model of the Basantapur Column evaluated the effect of column embedment depth and the related embedment joint stiffness (k_j) on the dynamic stability of the structure. Figure 10**Error! Reference source not found.**a shows that decreasing the embedment depth leads to an increase in the maximum rocking rotation of the column, while decreasing the joint stiffness at the embedment (in this case dividing it by factors of 10 and 100) also leads to a significant increase in the rocking response (Figure 10**Error! Reference source not found.**b). The extent to which these factors contributed to the response of the real structure cannot be conclusively determined without a more detailed

geotechnical investigation, but it is clear that rotation of the column due to embedment could well have increased the rocking response of the upper part of the structure. During the field survey, a gap was noticed between the base of the column and surrounding paving stones, indicating that some rotation of the embedded column did occur. This provides an additional explanation as to why the simulation results for the actual ground motion predict a marginally smaller response than the collapse that occurred.

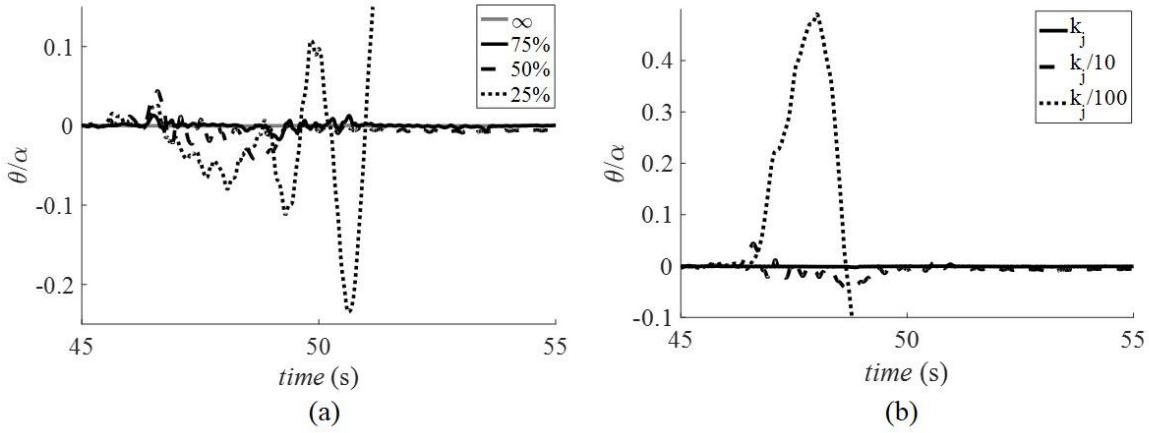

Figure 10. (a) Effect of embed depth on response (for case where joint stiffness is reduced by factor of 10) (b) Effect of joint stiffness on response (for 50% embedment case)

Dharahara Tower

In the case of the Dharahara Tower, the results from the computational analyses were compared both to the predictions of the analytical model, as well as corroborated with field observations, according to which the tower first cracked diagonally and rotated towards the south east, before eventually collapsing in a southwestern direction.

Effect of ground motion scaling and comparison with field observations

The first set of computational analyses evaluated the influence of ground motion scaling on the dynamic response of the tower. From this analysis it was found that when the acceleration data is scaled by a factor of 1.50, the computational model of the tower first rotates towards the northeast before a pulse in the opposite direction causes ground displacement towards the southwest, resulting in most of the debris falling in this direction (Figure 11**Error! Reference source not found.Error! Reference source not found.**) – which corresponds quite well with the final failure mode of the tower.

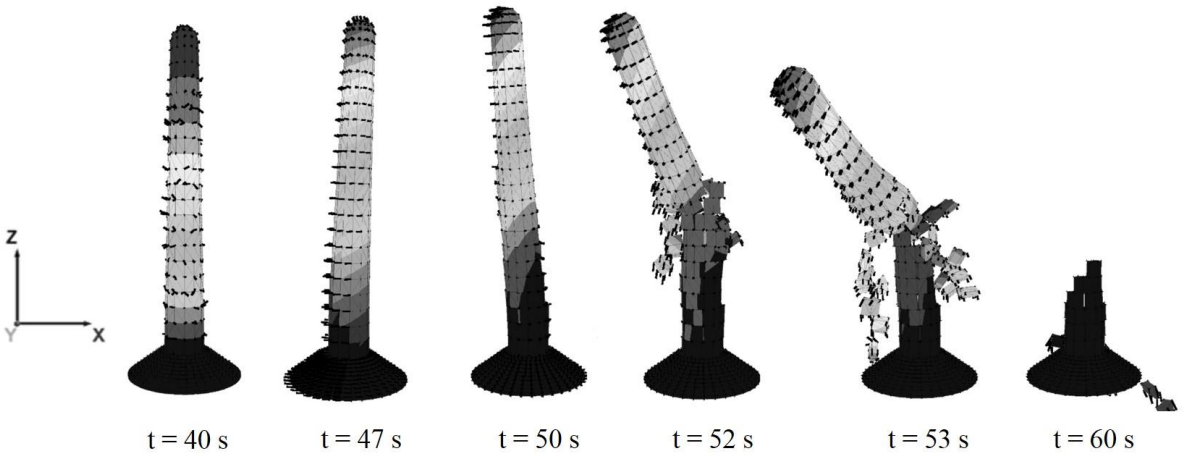

Figure 11. Progressive collapse of Dharahara Tower for ground motion scaling of 1.50

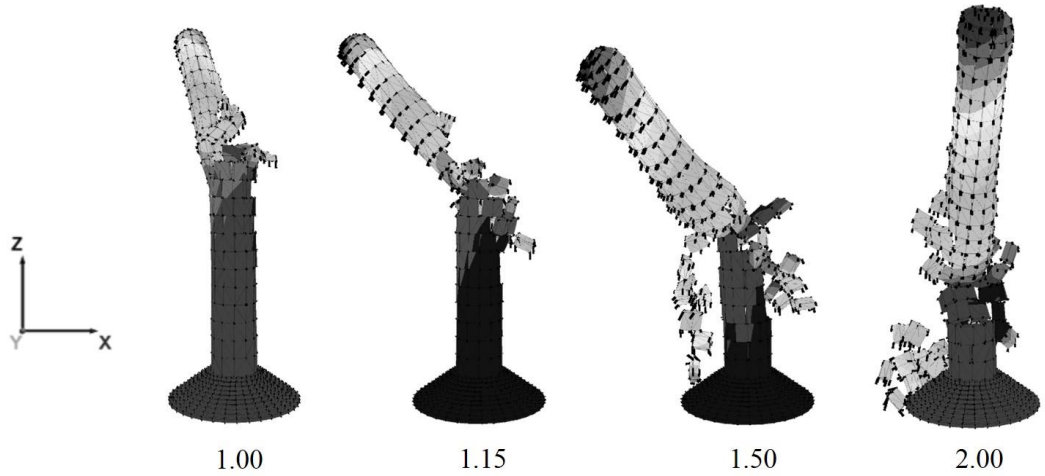

Figure 12. Comparison of failure modes for different ground motion scaling levels

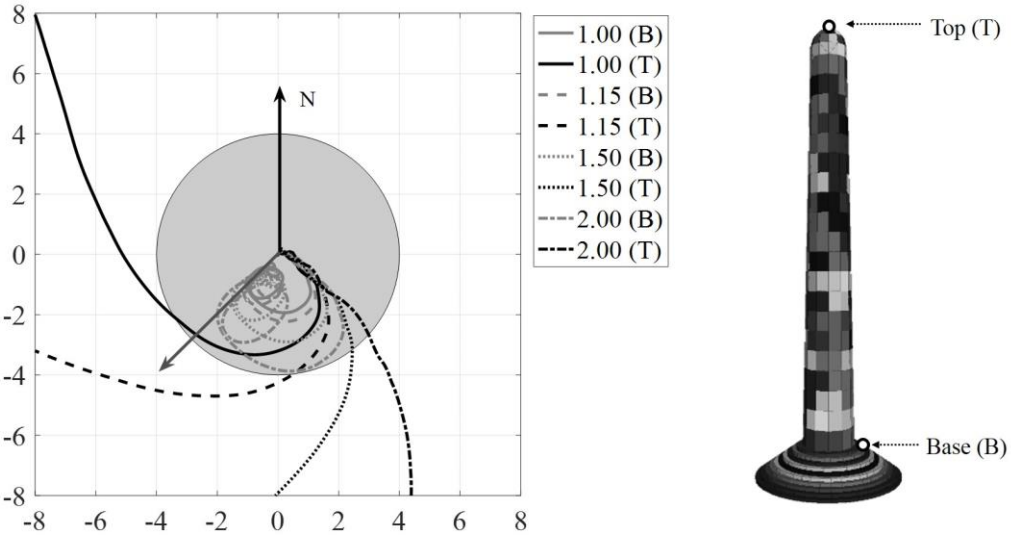

Figure 13. Effect of ground motion scaling (joint tensile strength = 1 kPa, grey arrow indicates actual collapse direction)

Varying the level of scaling of the earthquake ground motion was found to affect both the direction of collapse as well as the height at which the tower cracked – as illustrated by Figure 12**Error! Reference source not found.Error! Reference source not found.**. A decrease in ground motion scaling was observed to increase the height at which the crack occurred, and consequently decrease the size of the collapsed portion of the tower, while the direction of collapse appeared to follow a clockwise pattern – with the collapse direction progressively changing from southeast (for a scaling factor of 2) to northwest (scaling factor of 1).

As the Dharahara Tower experienced significant displacements in both cardinal directions, the time-history results are plotted in the form of displacement traces on a horizontal X-Y axis, as illustrated by Figure 13.**Error! Reference source not found.** The displacements are tracked at both the top center of the tower (T), as well as at the base (B) for the different levels of scaling of the earthquake ground motion. The diameter of the tower is also plotted in the form of a grey filled circle, which allows the magnitude of the displacements to easily be compared to the original diameter of the tower, while the grey arrow indicates the actual direction of collapse. From **Error! Reference source not found.**Figure 13 can be seen that for all ground motion scaling levels both the base and the top of the tower appear to follow a similar swirling pattern, with the displacement magnitude generally increasing with an increase in scaling. Furthermore the magnitude of the displacement at the bottom of the tower starts off as fairly large at first (and in the case of the scaling factor of 2 is almost equal to the radius of the tower) before gradually decreasing, while the response at the top continuously increases in magnitude. The dominant collapse directions for the different scaling levels are also more clearly indicated by Figure 13 **Error! Reference source not found.**- reiterating the observations from Figure 12**Error! Reference source not found.Error! Reference source not found.** about the different failure modes of the tower.

Parametric studies were also conducted to gauge the influence of joint tensile strength and the pedestal on the response of the tower. However, varying these parameters was found to have a relatively minor effect on the tower's dynamic behavior, and thus the results have not been presented here.

Comparison with analytical model

Since the mechanisms observed in 3DEC changed with varying ground motion scaling levels, comparisons could not be made with the analytical models in terms of maximum rotations. Instead, the rotations predicted by the analytical models in both cardinal directions were converted into the corresponding displacements at the top of the tower (relative to the base) and were compared to the 3DEC results for the same (Figure 14). From this plot it was found that the effect of simultaneously applying the ground motion in both cardinal directions was large – while both models started experiencing large displacements around the same time, the 3DEC models generally failed faster than their analytical counterparts, indicating it is possible that there was some interaction between the east-west and north-south components of the ground motion in 3DEC which affected the overall response of the tower, which was not included in the analytical model.

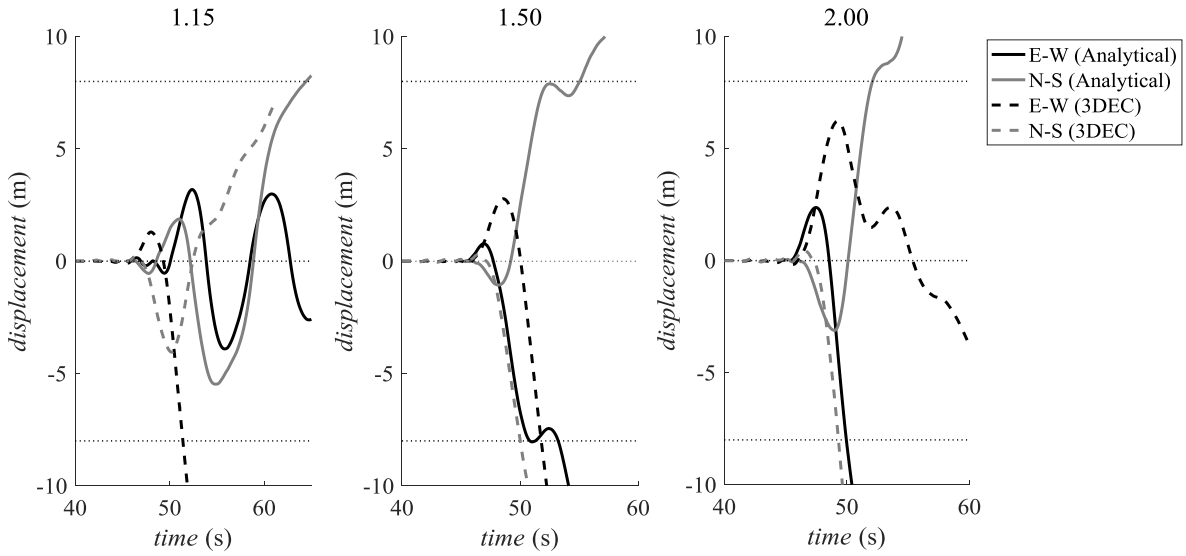

Figure 14. Comparison of 3DEC and analytical time-history results for the Dharahara Tower

DISCUSSION

IMPORTANCE OF GROUND MOTION PULSE

The resistance of objects to overturning is influenced by both their slenderness and size. While the slenderness of a structure determines when rocking initiates, the magnitude of rotation, and ultimately collapse, is governed by its size. Thus smaller objects can overturn without an obvious long duration pulse, while larger objects generally require a longer duration (lower frequency) pulse in order to generate enough rotational momentum to overturn and collapse – an observation which is also supported by the findings of this paper.

A comparison of the overturning plots for the selected structures reveals that the Dharahara Tower, with its considerably larger size, required a significantly longer pulse than any of the other monuments in order to overturn (Figure 15). In the case of the Nepal earthquake ground motion, the primary pulse alone was large enough to cause overturning of both the tower and the Basantapur Column, without taking into account any additional effects. Thus the large low-frequency content within the Nepal earthquake ground motion made slender unreinforced masonry structures particularly vulnerable to overturning, while structures of moderate size had their dynamic resistance almost completely eliminated by the long-duration pulse. In fact, any structure with a slenderness less than the amplitude of the dominant pulse extracted from the earthquake ground motion would have been in danger of collapse. Conversely, this could provide an explanation as to why the Narayan Temple, despite being of moderate size, did not overturn and collapse, as it was nearly twice as stocky as the tower, and 1.5 times as stocky as the column (Table 1). Essentially, the additional dynamic resistance to overturning typically characteristic of rocking motion (Doherty et al. 2002) was essentially non-existent for this particular ground motion. In other words, the Italian building code (NTC 2008) assessment method of predicting overturning to occur at ground accelerations equal to a multiple (typically 2) of the PGA, would have been extremely un-conservative here. The proper multiple would have been 1 for this earthquake, despite the fact that a value of 2 is usually conservative for typical ground motion recordings (particularly in Italy).

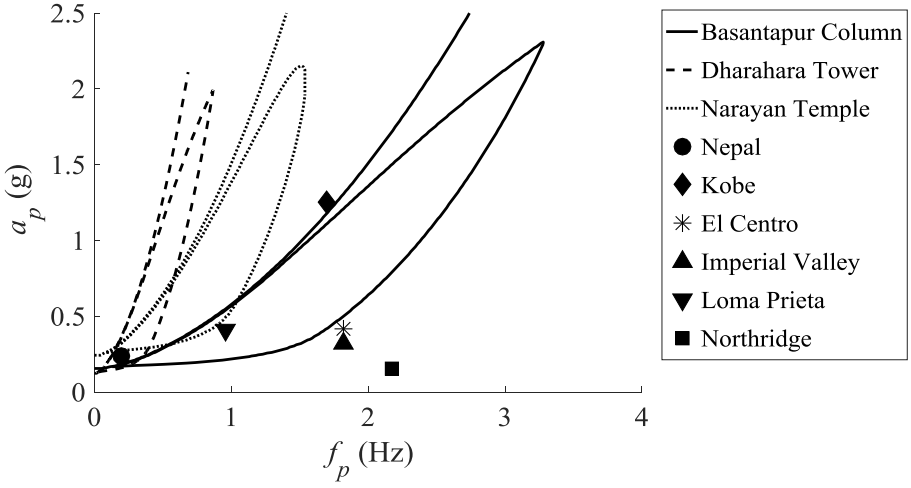

Figure 15. Comparison of the overturning plots for the selected monuments, and their predicted response to pulses isolated from different major earthquakes

This detrimental effect of the long-duration pulse present within the Nepal earthquake ground motion is better illustrated by comparing the predicted response of the three structures

to the primary pulses isolated from different major earthquakes. From Figure 15 it can be seen that despite their large magnitudes, none of the other earthquakes have a pulse large enough or long enough to cause the overturning of the Dharahara Tower or the Narayan Temple, and only a few have pulses long enough to cause the Basantapur Column to overturn. The scale effect becomes directly evident from this plot.

It should however be pointed out that this type of overturning failure is distinctly different from collapse caused by resonance, or by cumulative material failure causing excessive damage due to repeated cyclic loading. These types of failure are much more sensitive to the spectral acceleration at the natural frequencies of the structure. While elastic resonance can cause large base shears and subsequent damage, it cannot directly cause large rotations and overturning collapse. This provides some evidence as to the nature of the ground motion that caused only the top portion of the Dharahara Tower to collapse during the 1934 earthquake (as opposed to completely overturning around the base). Any distinct long-duration ground motion pulse, if present, would have had to have been of shorter period or lower amplitude than that observed in 2015. As a result, larger higher frequency excitation, accompanied by elastic amplification, might have played a larger role in the observed damage in 1934.

ELASTIC ANALYSIS OF THE DHARAHARA TOWER

Due to the size and slenderness of the Dharahara Tower, elastic effects might not have been negligible - thus an elastic analysis was also conducted wherein the possibility of elastic resonance due to modal amplification was investigated. Using Lord Rayleigh's principle, the natural frequency of the tower was calculated for the Young's modulus value specified in Table 2, as well as a range of density values, and was found to range between 0.64 – 0.83 Hz or 1.21 – 1.56 seconds, which is far from the 4 – 5 second dominant peak in the ground motion response spectra. Nevertheless, elastic resonance would have only initiated rocking earlier – it would not alone have caused complete overturning collapse about the base. This possibility of elastic resonance initiating rocking earlier, and consequently reducing the pulse amplitude required to cause collapse – especially in the region of the overturning plot where the Nepal earthquake pulse sits (Acikgoz and DeJong 2012) - also supports the result that the (analytical) time-history results were un-conservative.

The assumption of rigid blocks is less likely to be a source of error for the Basantapur Column however, as the response of the solid stone monument would probably be almost completely unaffected by elastic response.

EVALUATION OF ANALYTICAL TIME-HISTORY RESULTS

From the analytical time-history results it was found that while rocking generally initiated for the column and tower for all levels of scaling of the input ground motion, overturning only occurred for scaling factors of 1.15 and 1.50 and higher for the Basantapur Column and Dharahara Tower respectively (overturning of the tower for the scaling factor of 1.15 in the NS direction will be discussed separately). Similarly, rocking of the Narayan Temple only initiated for scaling factors of 1.50 and higher, with overturning of the structure only occurring when the ground motion was scaled by a factor of 2.00 or greater (Figure 7).

However, collapse of the column and tower (and initiation of rocking of the temple) obviously occurred for a scaling factor of 1, and the differences between the predictions of the time-history plots and what was observed in reality could be due to a number of factors. Firstly, the local ground motion at the site could have been different from what was recorded at the USGS KATNP and THM stations. All three monuments were situated in the Kathmandu Valley and would therefore have experienced similar long period effects, however they were separated by up to 12 km and could also have been subjected to local site effects. Furthermore, errors in estimating the mass and geometry of the structures when creating the Rhino models could have contributed to these discrepancies as well.

In the case of the Dharahara Tower, failure also involved some slipping of the tower off the pedestal which was not predicted in 3DEC due to the pre-defined block discretization which didn't allow a true diagonal crack as observed in reality. Additionally, due to the tower's size and slenderness, elastic effects as mentioned earlier might not have been negligible and could have decreased the pulse amplitude required for overturning to occur, while local crushing during rocking could have taken place as well. Furthermore, due to the soft soil in the Kathmandu Valley basin, soil-structure interaction effects might not have been negligible. In the case of the Basantapur Column, the embedment of the column in the ground was also observed to cause some rotation at the base which in turn affected overturning at the height at which it occurred. While this behavior was not reproduced analytically, the analyses conducted in 3DEC did corroborate these field observations.

COMPARISON OF ANALYTICAL TIME-HISTORY AND OVERTURNING PLOT RESULTS

A comparison between the analytical time-history responses and the predictions of the sine pulse overturning plots enables further discussion about the dominance of the long period pulse. For all three monuments there were instances when the overturning plots predicted collapse when the time-history analyses did not. Possible reasons for this follow.

Firstly, to extract the pulse information from the Nepal earthquake ground motion, a single sine pulse was fit to the most destructive pulse in the acceleration data. However the actual earthquake time-history contains higher frequency content, as well as several cycles of long-period motion as opposed to just a single pulse. Thus the presence of high frequency content combined with the imperfect fitting of the sine pulse could be one reason for the discrepancy between the time-history responses and predictions of the overturning plots.

Furthermore, the multiple cycles of long period pulses present in the acceleration data could have had an amplifying or de-amplifying effect on the response of the structure – depending on the phase of rocking relative to the ground motion. This behavior can be quantified in terms of the rate of energy input into the system (DeJong 2012a), which for the linearized equations of motion presented earlier (3,4) is:

$$\frac{\partial E}{\partial \tau} = -MR\ddot{u}_g\theta' \tag{6}$$

where E is the total energy, $\tau = pt$ is dimensionless time and θ' is the rotational velocity of the structure. From Equation 6 it can be seen that the rate of energy input is positive only if the current rotational velocity and ground motion are opposite in sign (DeJong 2012a). Thus maximum energy input (i.e. amplification resulting in overturning) is attained when the input ground motion (acceleration) is always opposite in sign to the rotational velocity, while removal of energy from the system (and subsequently de-amplification) takes place when the acceleration and rotational velocity are the same sign.

This de-amplifying effect is best illustrated by studying the response of the Dharahara Tower to the KATNP north-south ground motion record scaled by a factor of 1.25. As Figure 16a demonstrates, the rotational velocity and ground acceleration are initially perfectly out of phase, resulting in energy being input into the system thus causing an increase in the rocking amplitude of the tower. This is followed by a subsequent removal of energy from the system (de-amplification) by the pulse that followed, as a result of which the rocking amplitude of

the tower never exceeded 0.5α. Then, as the magnitude of the input acceleration decreased so did the rotation of the structure, resulting in a return to equilibrium despite the predictions of the overturning plot.

While rocking de-amplification can explain why the overturning plots predicted collapse while the time-history analyses did not, rocking amplification could account for those cases where the structure overturned faster than expected – as was observed for the Basantapur Column for scaling factors of 1.15, as well as for the Dharahara Tower for a scaling factor of 1.15 in the north-south direction (Figure 16b). As Figure 16b illustrates, the tower experienced some initial amplification between 45-55 seconds, which initiated the large rotation of the structure. This was followed by a second amplification between 57-60 seconds, which added energy to the system thus leading to the overturning of the tower for lower ground motion scaling than in Figure 16a.

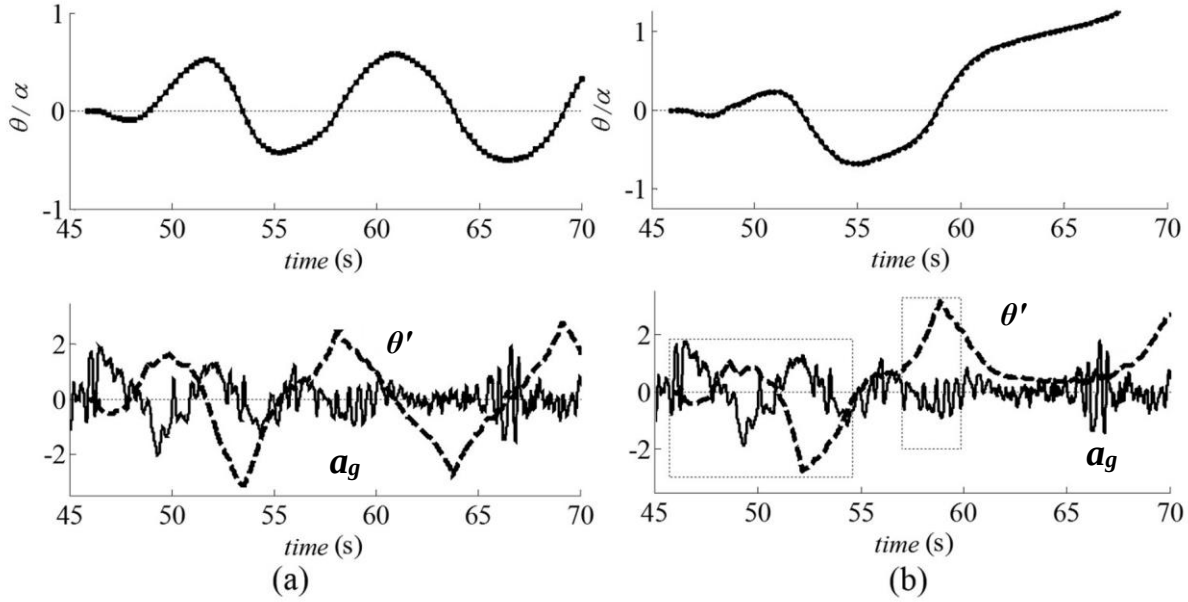

Figure 16. Comparison of the rotation (top), acceleration and angular velocity (bottom) time-histories for the Dharahara Tower: (a) scaling factor of 1.25; (b) scaling factor of 1.15

The similarity between Figures 16a & b indicates that once the large rocking response of the structure commences the overturning collapse can be very sensitive to the ground motion, with minor differences in phase affecting the outcome. For the most part however, the sine-pulse overturning envelopes were found to be sufficient for predicting the collapse of the three monuments, with the rest of the ground motion generally de-amplifying the rotation of the structure rather than amplifying it.

COMPARISON OF ANALYTICAL TIME-HISTORY AND 3DEC RESULTS

A comparison between the analytical time-history results and predictions of the computational (3DEC) model revealed a fairly good correlation between both sets of results for the Basantapur Column. For scaling factors of 1.15 and 1.50 the 3DEC and analytical results seemed to match almost exactly, while for the scaling factor of 1.25 the analytical model appeared to recover from a fairly large rotation before overturning about 2 seconds after the 3DEC model. This discrepancy could be due to the de-amplifying effect of the ground motion presented earlier, as well as the fact that both the north-south and east-west ground motion records were simultaneously applied to the computational model while the analytical model was subjected to the east-west ground motion record only.

CONCLUSIONS

This paper evaluated the performance of three historical structures which sustained varying levels of damage during the 2015 Gorkha earthquake. Analytical modelling of the structures using rocking dynamics revealed the importance of the large low frequency content within the Gorkha earthquake ground motion, as this is what caused larger structures such as the Dharahara Tower to overturn and fail. The overturning plots generated for each of the structures also illustrated the influence of size on stability, with smaller structures such as the Basantapur Column being far more vulnerable to collapse. Full time-history analyses were also conducted for different levels of scaling of the earthquake ground motion, and in the case of the Basantapur Column and Narayan Temple a fairly good correlation was observed between the predictions of the overturning plots and those of the time-history analyses. In the case of the Dharahara Tower however, the correlation was not as strong with the overturning plots yielding more conservative predictions than their time-history counterparts. Possible reasons for these discrepancies include elastic resonance in tower (which has the effect of decreasing the pulse amplitude required to cause overturning), as well as rocking de-amplification due to additional pulse cycles of the long-period ground motion.

Computational modelling of the column and tower was also conducted using discrete element modelling in 3DEC, with the objective of capturing certain features of the dynamic response not considered by the analytical models. In the case of the column this included rocking of the embedded part of the column, which was also observed during the field survey. In the case of the Dharahara Tower, this included identification of a swirling

displacement that led to collapse when both components of the horizontal ground motion were considered, highlighting the 3D nature of the response.

REFERENCES

Acikgoz, S., and DeJong, M.J., 2012. The Interaction of Elasticity and Rocking in Flexible Structures Allowed to Uplift, *Earthquake Engineering & Structural Dynamics* **41**, 2177–94.

Atkinson, R.H., Amadei, B.P., Saeb, S., and Sture, S., 1989. Response of Masonry Bed Joints in Direct Shear, *Journal of Structural Engineering* **115**, 2276–96.

Aydan, Ö., and Ulusay, R., 2015. *A Quick Report on the 2015 Gorkha (Nepal) Earthquake and Its Geo-Engineering Aspects.*

Barton, N.R., 1976. The Shear Strength of Rock and Rock Joints, *International Journal of Rock Mechanics and Mining Sciences* **13**, 255–79.

Bui, T.T., and Limam, A., 2012. Masonry Walls under Membrane or Bending Loading Cases : Experiments and Discrete Element Analysis, Paper No. 119, in *Proceedings of the Eleventh International Conference on Computational Structures Technology*, 4-7 September, 2012, Drubnovik, Croatia.

Capozucca, R., 2011. Shear Behaviour of Historic Masonry Made of Clay Bricks, *The Open Construction and Building Technology Journal* **5**, 89–96.

de Felice, G., and Giannini, R., 2000. Assessment of Seismic Vulnerability to Out-of-Plane Collapse of Masonry Walls, Paper No. 0715, in *Proceedings of the 12th World Conference on Earthquake Engineering*, 30 January – 4 February, 2000, Auckland, New Zealand.

De Lorenzis, L., DeJong, M.J., and Ochsendorf, J.A., 2007. Failure of Masonry Arches under Impulse Base Motion, *Earthquake Engineering & Structural Dynamics* **36**, 2119–36.

DeJong, M.J., 2009. Seismic Assessment Strategies for Masonry Structures, Ph.D. Thesis, Massachusetts Institute of Technology.

DeJong, M.J., 2012a. Amplification of Rocking Due to Horizontal Ground Motion, *Earthquake Spectra* **28**, 1405–21.

DeJong, M.J., 2012b. Seismic Response of Stone Masonry Spires: Analytical Modeling, *Engineering Structures* **40**, 556–65.

DeJong, M.J., and Dimitrakopoulos, E.G., 2014. Dynamically Equivalent Rocking Structures, *Earthquake Engineering & Structural Dynamics* **43**, 1543–63.

DeJong, M.J., and Vibert, C., 2012. Seismic Response of Stone Masonry Spires: Computational and Experimental Modeling, *Engineering Structures* **40**, 566–74.

Dimitrakopoulos, E.G., and DeJong, M.J., 2012. Revisiting the Rocking Block: Closed-Form Solutions and Similarity Laws, *Proceedings of the Royal Society A: Mathematical, Physical and Engineering Sciences* **468**, 2294–2318.

Dixit, A.M. et al., 2015. Strong-Motion Observations of the M 7.8 Gorkha, Nepal, Earthquake Sequence and Development of the N-SHAKE Strong-Motion Network, *Seismological Research Letters* **86**, 1533–39.

Doherty, K. et al., 2002. Displacement-Based Seismic Analysis for out-of-Plane Bending of Unreinforced Masonry Walls, *Earthquake Engineering & Structural Dynamics* **31**, 833–50.

Drysdale, R.G., Vanderkeyl, R., and Hamid, A.A., 1979. Shear Strength of Brick Masonry Joints, in *Proceedings, 5th International Brick Masonry Conference*, 5-10 October, 1979, Washington DC.

Galetzka, J. et al., 2015. Slip Pulse and Resonance of Kathmandu Basin during the 2015 Gorkha Earthquake Nepal, *Science* **349**, 1091–95.

Gazetas, G. et al., 2012. Sliding and Overturning Potential of Christchurch 2011 Earthquake Records, *Earthquake Engineering & Structural Dynamics* **41**, 1921–44.

Goda, K. et al., 2015. The 2015 Gorkha Nepal Earthquake: Insights from Earthquake Damage Survey, *Frontiers in Built Environment* **1**, 1–15.

Hayes, G.P. et al., 2015. Rapid Characterization of the 2015 M_w 7.8 Gorkha, Nepal, Earthquake Sequence and Its Seismotectonic Context, *Seismological Research Letters* **86**, 1557–67.

Housner, G.W., 1963. The Behavior of Inverted Pendulum Structures during Earthquakes, *Bulletin of the Seismological Society of America* **53**, 403–17.

Itasca Consulting Group, 2007. *3DEC - 3 Dimensional Distinct Element Code*, software, http://www.itascacg.com/software/3dec.

Kaushik, H.B., Rai, D.C., and Jain, S.K., 2007. Stress-Strain Characteristics of Clay Brick Masonry under Uniaxial Compression, *Journal of Materials in Civil Engineering* **19**, 728–39.

Makris, N., and Konstantinidis, D., 2001. *The Rocking Spectrum and the Shortcomings of Design Guidelines, Report No. PEER-01/07*, Berkeley, CA.

Makris, N., and Roussos, Y., 2000. Rocking Response of Rigid Blocks under near-Source Ground Motions, *Geotechnique* **50**, 243–62.

Makris, N., and Zhang, J., 1999. *Rocking Response and Overturning of Anchored Equipment under Seismic Excitations, Report No. PEER-98/05*, Berkeley, CA.

Martin, S.S., Hough, S.E., and Hung, C., 2015. Ground Motions from the 2015 Mw 7.8 Gorkha, Nepal, Earthquake Constrained by a Detailed Assessment of Macroseismic Data, *Seismological Research Letters* **86**, 1524–32.

Mehrotra, A., Arêde, A., and DeJong, M.J., 2015. Discrete Element Modeling of a Post-Tensioned Masonry Arch, Paper No. 49, in *Proceedings of the 15th International Conference on Civil, Structural and Environmental Engineering Computing*, 1-4 September, 2015, Prague, Czech Republic.

Menon, A. et al., 2017. Field Observations on the Performance of Heritage Structures in the Nepal 2015 Earthquake, Paper No. 2465, in *Proceedings of the 16th World Conference on Earthquake Engineering*, 9-13 January, 2017, Santiago, Chile.

National Planning Commission (NPC), 2015. *Nepal Earthquake 2015: Post Disaster Needs Assessment, Executive Summary*.

NTC, 2008. Norme Tecniche per Le Costruzioni. Ministry of Infrastructures and Transportations, 4 February 2008, *G.U.S.O No. 30*, Rome.

Papantonopoulos, C. et al., 2002. Numerical Prediction of the Earthquake Response of Classical Columns Using the Distinct Element Method, *Earthquake Engineering and Structural Dynamics* **31**, 1699–1717.

Papastamatiou, D.Y., and Psycharis. I.N., 1993. Seismic Response of Classical Monuments-a Numerical Perspective Developed at the Temple of Apollo in Bassae, Greece, *Terra Nova* **5**, 591–601.

Parajuli, R.R., and Kiyono, J., 2015. Ground Motion Characteristics of the 2015 Gorkha Earthquake, Survey of Damage to Stone Masonry Structures and Structural Field Tests, *Frontiers in Built Environment* **1**, 1–12.

Rai, D.C., and Dhanapal, S., 2013. Bricks and Mortars in Lucknow Monuments of C. 17-18 Century, *Current Science* **104**, 238–44.

730 Roberti, G.M., and Calvetti, F., 1998. Distinct Element Analysis of Stone Arches, in *Arch Bridges* (A
731 Sinopoli, ed.), A.A. Balkema, Rotterdam, 181–86.

732 Stockl, S., and Hofmann, P., 1986. Tests on the Shear Bond Behaviour in the Bed-Joints of Masonry,
733 *Masonry International*, 292–303.

734 Takai, N. et al., 2016. Strong Ground Motion in the Kathmandu Valley during the 2015 Gorkha,
735 Nepal, Earthquake, *Earth, Planets and Space* **68**, 10.

736 Tallet-Williams, S. et al., 2016. Site Amplification in the Kathmandu Valley during the 2015 M7.6
737 Gorkha, Nepal Earthquake, *Bulletin of Earthquake Engineering* **14**, 3301–15.

738 Yim, C.S., Chopra, A.K., and Penzien, J., 1980. Rocking Response of Rigid Blocks to Earthquakes,
739 *Earthquake Engineering & Structural Dynamics* **8**, 565–87.

740 Zhang, P, and Makris, N., 2001. Rocking Response of Free-Standing Blocks under Cycloidal Pulses,
741 *Journal of Engineering Mechanics* **127**, 473–83.